

Control of excitons by laterally modulated electrode density

Y. Y. Kuznetsova,^{a)} A. A. High, and L. V. Butov

Department of Physics, University of California at San Diego, La Jolla, California 92093-0319, USA

(Received 30 September 2010; accepted 20 October 2010; published online 18 November 2010)

We propose a method for the realization of in-plane potential landscapes for excitons by the lateral modulation of the electrode density and present traps created using this method. © 2010 American Institute of Physics. [doi:10.1063/1.3517444]

An indirect exciton in a coupled quantum well (CQW) structure is composed of an electron and a hole in spatially separated QWs [Fig. 1(a)]. The spatial separation leads to a long exciton lifetime, allowing indirect excitons to cool below the temperature of quantum degeneracy, and thus providing the opportunity to study the physics of cold excitons. Furthermore, indirect excitons have a built-in dipole moment ed , where d is the separation between the electron and hole layers, so their energy can be controlled by voltage: an electric field F_z perpendicular to the QW plane results in the exciton energy shift $E=edF_z$.¹ This gives an opportunity to create in-plane potential landscapes for excitons $E(x,y)=edF_z(x,y)$. Advantages of electrostatically created potential landscapes include the opportunity to realize the desired potential profile and control it *in situ*, on time scale shorter than the exciton lifetime. Excitons were studied in various potential landscapes created by laterally modulated voltage $V(x,y)$: ramps,^{2,3} lattices,⁴⁻⁷ traps,⁷⁻¹¹ and circuit devices.¹²⁻¹⁵

Potential traps are an effective tool for studying the physics of cold gases. For instance, they made the achievement of atomic Bose-Einstein condensation (BEC) possible.^{16,17} Traps can become an effective tool for studying the physics of cold excitons.

The potential profile of a trap is crucial for the trap performance. The quantum degeneracy of an exciton gas can be achieved in a paraboliclike trap, which can collect excitons from a large area to the trap center. A circular electrode can produce a confining in-plane potential on a small area only.¹¹ In an effort to create larger traps with confining potentials, diamond traps were developed.¹¹ The diamond trap is formed by a diamond-shaped top electrode, which produces a paraboliclike confining potential.¹¹ However, the area of the diamond traps was still limited to about $40 \mu\text{m}^2$.

In this work, we present a method for the realization of in-plane potential landscapes for excitons. The principle of this method is presented in Fig. 1. The potential landscapes for excitons are created by a single shaped electrode with laterally modulated electrode density. The divergence of the electric field at the electrode edges results in the reduction of its normal component F_z . This gives an opportunity to control F_z by adjusting the electrode density. Figure 1(d) demonstrates this principle with a square grid electrode [Fig. 1(c)]. The electrode density is varied by changing the line thickness and hole size. F_z decreases for lower electrode densities, resulting in the required control of the exciton energy [Fig. 1(d)].

A substantial variation of the exciton energy [Fig. 1(d)] can be achieved (i) with a small applied voltage ($V=1$ V for the data in Fig. 1), (ii) with a small in-plane variation of the exciton energy (significantly smaller than a typical in-plane disorder ~ 1 meV in high-quality QW samples) [Fig. 1(e)], and (iii) keeping in-plane electric field F_{xy} small so that it does not cause the exciton dissociation [Fig. 1(f)]. Indeed, for all the data in Fig. 1, $eF_{xy}a_B \ll E_{ex}$ ($a_B \sim 20$ nm and $E_{ex} \sim 4$ meV are the Bohr radius and binding energy for the indirect excitons in the CQW,^{18,19} respectively), i.e., F_{xy} remains well below the threshold for the exciton dissociation.¹

We modeled the potential energy profiles of electrostatic traps by numerically solving Poisson's equation and thus calculating the electric field as a function of position for various electrode shapes. The calculations are performed for the following parameters of the CQW structure: $d=12$ nm, the distance between the top shaped electrode and the bottom homogeneous electrode $D=1 \mu\text{m}$, CQW is positioned 100 nm above the bottom electrode. Positioning the CQW layers

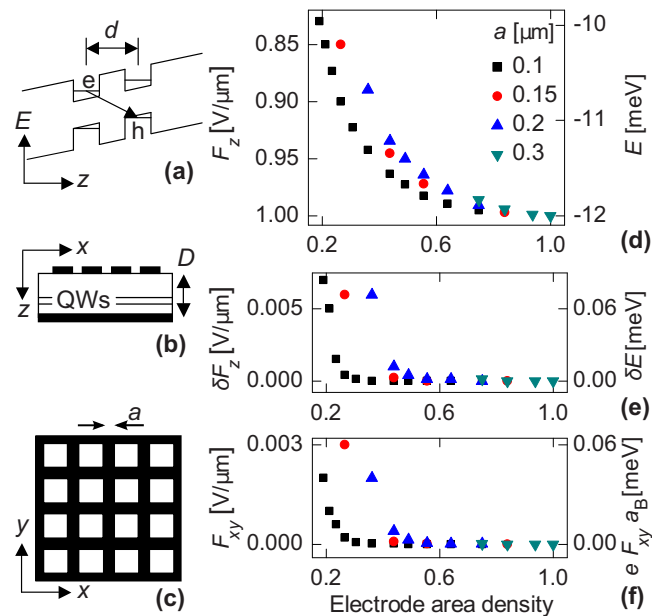


FIG. 1. (Color online) The principle of control of exciton energy by electrode density. (a) CQW diagram. (b) Schematic of the sample with a ground plane at the bottom and an electrode pattern at the top. (c) Schematic of a top square grid electrode used in the calculations in (d)–(f). (d) The electric field in the z -direction F_z and exciton energy E as a function of the area density of the square grid electrode for different widths a of the grid lines. (e) The lateral variation of F_z and E . (f) The in-plane electric field F_{xy} and $eF_{xy}a_B$, where a_B is the exciton Bohr radius. $V=1$ V, $d=12$ nm, $D=1 \mu\text{m}$, and the CQW is positioned 100 nm above the homogeneous bottom electrode in the calculations.

^{a)}Electronic mail: yuliyakuzn@gmail.com.

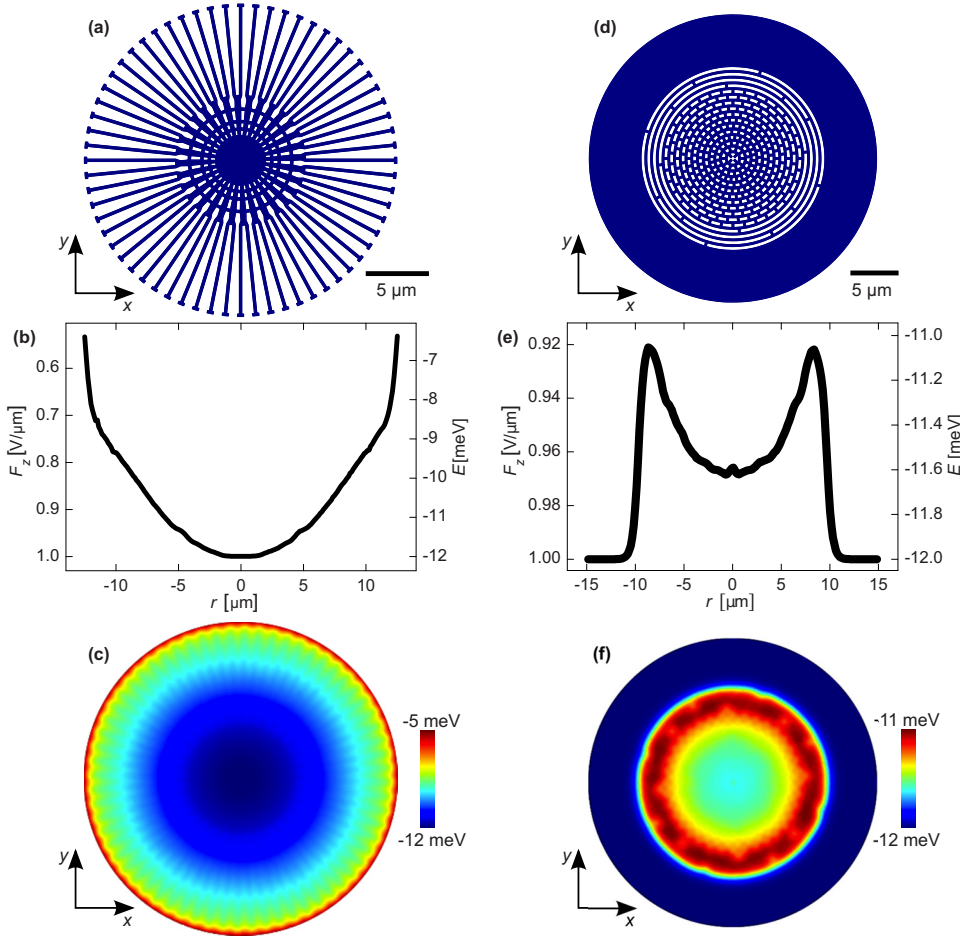


FIG. 2. (Color online) Snowflake traps. [(a)–(c)] Parabolic trap. [(d)–(f)] Elevated trap. [(a) and (d)] The top electrode. [(b) and (e)] The radial profile of the electric field in the z -direction F_z and exciton energy E . The azimuthal variation of F_z and E is within the line thickness. [(c) and (f)] x - y profile of the exciton energy in the trap. The in-plane electric field $F_{xy} < 0.01$ V/ μm for both traps. $V = 1$ V, $d = 12$ nm, $D = 1$ μm , and the CQW is positioned 100 nm above the homogeneous bottom electrode in the calculations.

closer to the homogeneous bottom electrode allows lowering F_{xy} .⁷ These parameters are typical for CQW structures;^{6,7,10–15} $d = 12$ nm corresponds to a CQW structure with 8 nm QWs separated by a 4 nm barrier. The calculations are performed for $V = 1$ V applied to the top electrode, while the bottom electrode is grounded [Fig. 1(b)]. This creates an in-plane potential landscape for indirect excitons $E(x, y) = eF_z(x, y)$. The applied voltage controls the amplitude of the potential landscape.

Using this method, a two-dimensional parabolic trap was modeled. Increasing the electrode density toward the trap center results in the exciton potential energy eF_z being the deepest at the trap center and progressively shallower toward the edge. The top electrode that creates this potential has a “snowflake” shape shown in Fig. 2(a). The electrode shape was designed to realize a two-dimensional parabolic potential [Fig. 2(b)]. The azimuthal variation of F_z and, in turn, the exciton energy are small, within the line thickness for the curve plotted in Fig. 2(b). The in-plane electric field F_{xy} is less than 0.01 V/ μm for the entire trap, well below the threshold of exciton dissociation: $eF_{xy}a_B < 0.2$ meV is small compared to the exciton binding energy, 4 meV. The “snowflake trap” provides a strong in-plane confinement for excitons: its depth is about 5 meV for $V = 1$ V.

Such “snowflake traps” and other potential landscapes for excitons formed by laterally modulated electrode density have the following advantages: (i) they allow the realization of a confining in-plane potential for excitons on a large area, about ten times greater than the area achieved in the diamond traps. This results in a significant enhancement of the number

of excitons that can be collected to the trap center and form a high-density exciton gas, a requirement for the achievement of quantum degeneracy and exciton BEC. In addition, due to the effective collection of excitons to the trap center, a weak excitation power can be used to achieve a high exciton density. This suppresses the effect of heating due to excitation. (ii) The heating of excitons by in-plane currents, which can appear due to in-plane voltage gradients in earlier excitonic devices created by laterally modulated voltage, is also suppressed in snowflake landscapes because the electrode is held at a single voltage. (iii) Advantages of the snowflake trap also include the simplicity of fabrication and accuracy of control. Switching off the trap potential, like in atomic time-of-flight experiments, or modulating trap depth, like in atomic collective mode experiments,^{16,17} can be realized by modulating a single electrode voltage.

The method allows creating a variety of in-plane potential landscapes for excitons. See Fig. 2 and supplementary material²⁰ for a few examples. Supplemental Fig. 1 presents a one-dimensional counterpart of the parabolic snowflake trap—a guiding channel for excitons. The widths of the strips and spacing between them can be adjusted to produce a potential profile of the desired shape, a parabolic guiding channel in the presented case.

Figures 2(d)–2(f) present an elevated trap. Elevated traps can be used for evaporative cooling of excitons. As described in Refs. 10 and 11, high-energy excitons are more likely than low-energy excitons to escape from the trap over the barrier, increasing the relative population of low-energy excitons left in the trap. This evaporative cooling can lower the effective

temperature of excitons in the trap, thus facilitating the achievement of quantum degeneracy in the trapped exciton gas.

The escape of high-energy excitons at the trap edges may become less effective for large traps. Evaporative cooling can be facilitated by introducing evaporative cooling sites inside the trap. Supplemental Fig. 2 presents an example of such evaporative cooling site. Here, more energetic excitons can overcome the barrier and fall into the cooling site, thus escaping the trap and leaving lower-energy excitons in the trap.

In conclusion, we demonstrated a principle of control of exciton energy by electrode density. We presented potential landscapes created using this principle, including traps for collecting excitons from a large area to the trap center, guiding channels for excitons, and elevated traps for excitons.

We thank A. C. Gossard, A. T. Hammack, J. R. Leonard, and M. Remeika for the discussions. This work was supported by US ARO under award W911NF-08-1-0341

¹D. A. B. Miller, D. S. Chemla, T. C. Damen, A. C. Gossard, W. Wiegmann, T. H. Wood, and C. A. Burrus, *Phys. Rev. B* **32**, 1043 (1985).

²M. Hagn, A. Zrenner, G. Böhm, and G. Weimann, *Appl. Phys. Lett.* **67**, 232 (1995).

³A. Gärtner, A. W. Holleitner, J. P. Kotthaus, and D. Schuh, *Appl. Phys. Lett.* **89**, 052108 (2006).

⁴S. Zimmermann, A. O. Govorov, W. Hansen, J. P. Kotthaus, M. Bichler,

and W. Wegscheider, *Phys. Rev. B* **56**, 13414 (1997).

⁵J. Krauß, J. P. Kotthaus, A. Wixforth, M. Hanson, D. C. Driscoll, A. C. Gossard, D. Schuh, and M. Bichler, *Appl. Phys. Lett.* **85**, 5830 (2004).

⁶M. Remeika, J. C. Graves, A. T. Hammack, A. D. Meyertholen, M. M. Fogler, L. V. Butov, M. Hanson, and A. C. Gossard, *Phys. Rev. Lett.* **102**, 186803 (2009).

⁷A. T. Hammack, N. A. Gippius, S. Yang, G. O. Andreev, L. V. Butov, M. Hanson, and A. C. Gossard, *J. Appl. Phys.* **99**, 066104 (2006).

⁸T. Huber, A. Zrenner, W. Wegscheider, and M. Bichler, *Phys. Status Solidi A* **166**, R5 (1998).

⁹G. Chen, R. Rapaport, L. N. Pfeiffer, K. West, P. M. Platzman, S. Simon, Z. Vörös, and D. Snoke, *Phys. Rev. B* **74**, 045309 (2006).

¹⁰A. A. High, A. T. Hammack, L. V. Butov, L. Mouchliadis, A. L. Ivanov, M. Hanson, and A. C. Gossard, *Nano Lett.* **9**, 2094 (2009).

¹¹A. A. High, A. K. Thomas, G. Grosso, M. Remeika, A. T. Hammack, A. D. Meyertholen, M. M. Fogler, L. V. Butov, M. Hanson, and A. C. Gossard, *Phys. Rev. Lett.* **103**, 087403 (2009).

¹²A. A. High, A. T. Hammack, L. V. Butov, M. Hanson, and A. C. Gossard, *Opt. Lett.* **32**, 2466 (2007).

¹³A. A. High, E. E. Novitskaya, L. V. Butov, M. Hanson, and A. C. Gossard, *Science* **321**, 229 (2008).

¹⁴G. Grosso, J. Graves, A. T. Hammack, A. A. High, L. V. Butov, M. Hanson, and A. C. Gossard, *Nat. Photonics* **3**, 577 (2009).

¹⁵Y. Y. Kuznetsova, M. Remeika, A. A. High, A. T. Hammack, L. V. Butov, M. Hanson, and A. C. Gossard, *Opt. Lett.* **35**, 1587 (2010).

¹⁶E. A. Cornell and C. E. Wieman, *Rev. Mod. Phys.* **74**, 875 (2002).

¹⁷W. Ketterle, *Rev. Mod. Phys.* **74**, 1131 (2002).

¹⁸M. M. Dignam and J. E. Sipe, *Phys. Rev. B* **43**, 4084 (1991).

¹⁹M. H. Szymanska and P. B. Littlewood, *Phys. Rev. B* **67**, 193305 (2003).

²⁰See supplementary material at <http://dx.doi.org/10.1063/1.3517444> for simulation details, guiding channel, and evaporative cooling site.

Copyright 2010 American Institute of Physics. This article may be downloaded for personal use only. Any other use requires prior permission of the author and the American Institute of Physics.

The following article appeared in Appl. Phys. Lett. 97, 201106 and may be found at <http://link.aip.org/link/?APL/97/201106>.